

Angle matching in intravascular elastography

C.R.M. Janssen ^{a,b}, C.L. de Korte ^{a,*}, M.S. van der Heiden ^b, C.P.A. Wapenaar ^a,
A.F.W. van der Steen ^{a, c}

^a Thoraxcenter, Erasmus University Rotterdam, Rotterdam, The Netherlands

^b Laboratory of Seismics and Acoustics, Delft University of Technology, Delft, The Netherlands

^c Interuniversity Cardiology Institute of the Netherlands, The Netherlands

Abstract

Intravascular elastography is a new technique to obtain mechanical properties of the vessel wall and plaque. Mechanical information of vascular tissue is important for characterisation of different plaque components, detection of plaque vulnerability and thus choosing the proper interventional technique. The feasibility of the technique is investigated using phantoms and diseased human arteries. These studies demonstrated that elastography reveals information that is unavailable or inconclusive from the echogram alone.

The technique is based on the principle that tissue strain is directly related to its mechanical properties. In intravascular elastography, the tissue is compressed using different intravascular pressures. The strain is determined using cross-correlation techniques of the radio frequency (r.f.) signals. Reliable strain estimates are only obtained when signals of corresponding tissue are correlated. Owing to catheter motion, off-centre position and non-uniform rotation of the intravascular transducer, the r.f. traces at low and at high pressure may be misaligned.

Four algorithms are tested to track the corresponding ultrasound signals. Three methods (I_1 norm, I_2 norm and cross-correlation) are applied on the r.f. signal and one (I_1 norm) on the envelope (speckle tracking). Simulations are performed to obtain a data set with a priori knowledge of the scattering particles positions in the tissue at high and low pressure. Different positions of the catheter in the lumen, compression levels of the material and signal-to-noise ratios (SNRs) are investigated. Finally, these findings are corroborated with a phantom experiment in a water tank.

From the simulations, it can be concluded that the speckle tracking algorithm has the best performance, under all circumstances. The performance decreases with larger eccentricity of the catheter and larger compression of the material. The SNR is only of minor influence. The speckle tracking algorithm has also the best performance in the phantom experiment.

The performance of the speckle tracking algorithm is better than the three r.f.-based algorithms. For intravascular elastography, implementation of this method may improve the quality of the elastogram. © 2000 Elsevier Science B.V. All rights reserved.

Keywords: Intravascular elastography; Plaque; Speckle tracking algorithm

1. Introduction

Coronary atherosclerosis is one of the leading causes of hospitalisation in the western world. Blood vessel obstructions are caused by atherosclerosis and may result in the loss of vital functions. Diagnostic intravascular ultrasound (IVUS) imaging systems have been developed in the past few years to support the clinical treatment of this obstructive vascular disease.

Intravascular elastography is a new technique to

obtain the local mechanical properties of the vessel wall and its pathology using IVUS. Because soft materials support larger strains than hard, measurement of the strain can be used to distinguish tissues with different stiffnesses. Knowing the relative stiffness of atherosclerotic lesions can help physicians in the selection of the most appropriate therapeutic modality. Intravascular elastography studies have been performed in human arteries in vitro [1]. Qualitative comparison of the elastograms and the histology demonstrates the potential of intravascular elastography to obtain mechanical information of the vessel wall and the plaque. The strain elastograms reveal useful information that is not obtained from IVUS alone.

An elastogram is produced following steps I, II, III

* Corresponding author. Mailing address: Exp. Echo Ee 23.02, Erasmus University, PO Box 1738, 3000 DR Rotterdam, The Netherlands. Tel.: +31-10-4088033; fax: +31-10-4089445.

E-mail address: dekorte@tch.fgg.eur.nl (C.L. de Korte)

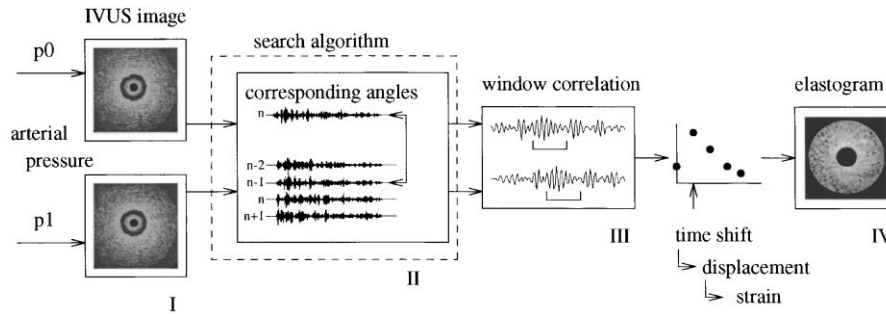


Fig. 1. Processing flow diagram to produce an elastogram.

and IV of the processing flow diagram as shown in Fig. 1. A stepper motor rotates an intravascular catheter over 400 angles per revolution. Two IVUS images at two different pressures are acquired (I). The next step (II) is finding the corresponding angles with the help of a search algorithm, which looks for the global similarity between two signals. The following step is correlating windows to calculate the local time shifts between the r.f. signals acquired at the different pressure levels (III). Finally, these time shifts are converted into strain values by taking the two point finite difference and an elastogram is produced by plotting these strain values in grey levels (IV).

Since the local strain is determined using a trace-to-trace algorithm (III), it is essential that traces imaging the same tissue are correlated (II). Owing to the movement of the catheter, rotational artefacts caused by the flexible shaft of the catheter or an eccentric position of the catheter, the alignment of traces can be affected. Therefore it is necessary to determine which windows have to be correlated with each other. This requires a method that searches for similarity in the signals.

In this study these methods are called search algorithms. These methods search which window of a trace in the data set acquired at the low pressure belongs to which window of a trace in the data set acquired at the high pressure. The performance of four methods to match corresponding traces is investigated in this study using simulations and phantom experiments.

2. Methods

2.1. Search algorithms

Four possible search algorithms are presented. A subset of search algorithms can be described by the l_n norm. The general formula for the l_n norm to compare two signals is

$$\|x(k, l)\|_n = n \sqrt[n]{\sum_{i=1}^N |y_{i+k, l} - x_i|^n}, \quad (1)$$

where x_i is the i th sample point of a window of the

signal at low pressure and y_i is the i th sample point of a window of the signal at high pressure. The signals are subtracted over a time interval $i=1$ till N . To compare the signals, y_i is shifted k sample points and l angles in relation to x_i , in intervals between -10 and 50 , and between -5 and 5 , respectively. The n defines the norm. If the substitution $n=1$ is made, Eq. (1) is defined as the l_1 norm:

$$\|x(k, l)\|_1 = \sum_{i=1}^N |y_{i+k, l} - x_i|. \quad (2)$$

This algorithm, also called the SAD algorithm (sum absolute difference) subtracts two signals and computes the sum of the absolute differences for all the time samples. The minimum of these sums, calculated for all k and l indicates the best match [2–5].

The second algorithm, the l_2 norm, is obtained from Eq. (1), if n is set to 2 ($n=2$):

$$\|x(k, l)\|_2 = \sqrt{\sum_{i=1}^N |y_{i+k, l} - x_i|^2}. \quad (3)$$

In this case the subtracted amplitudes are first squared, before they are summed. The best match of the two signals at different pressures is obtained by looking for the minimum of the squared roots [3,5]. The l_2 norm is known as the least square error.

Another algorithm is the cross-correlation function. The standard correlation coefficient used to express the association between two random variables X and Y is given as

$$R = \frac{\sigma_{xy}}{\sigma_x \sigma_y}, \quad (4)$$

where σ_x is the standard deviation of X , σ_y is the standard deviation of Y and σ_{xy} is the covariance of X and Y . R is the normalised cross-correlation coefficient such that $-1 \leq R \leq +1$, where $R = -1$ indicates a perfect negative association, $R = +1$ represents a perfect positive association and $R = 0$ indicates that no association exists between X and Y . In the case where X consists of N discrete values and Y of M discrete values ($M > N$) such that $X = x_1, x_2, x_3, \dots, x_N$ and $Y = y_1, y_2, y_3, \dots$,

y_M , the correlation coefficient can be written as

$$R(k, l) = \frac{\sum_{i=1}^N (x_i - \bar{X})(y_{i+k, l} - \bar{Y})}{\sqrt{\sum_{i=1}^N (x_i - \bar{X})^2 \sum_{i=1}^N (y_{i+k, l} - \bar{Y})^2}}, \quad (5)$$

where \bar{X} is the mean of X and \bar{Y} is the mean of Y [2,4,5]. If X and Y are two ultrasound echoes that have been digitised and stored, then Eq. (5) can be used to determine the similarity between the two ultrasound echoes. One signal is shifted, and the cross-correlation coefficient is calculated again. The maximum of the cross-correlation coefficients is an indication for the best match.

The last algorithm is called speckle tracking. This algorithm uses the envelope of the r.f. signals before using one of the aforementioned algorithms. The absolute value of the analytical signal is taken to get the envelope of a signal. This algorithm smooths a signal and has less resolution, because it does not use the detailed r.f. signal. From now on the l_1 norm applied to the envelope of the signal is called the speckle tracking algorithm.

2.2. Simulation

For testing the performance of the algorithms a priori knowledge is necessary concerning the best match of the set of signals. A computer simulation is a good solution, because all the variables are controllable; the simulated phantom expands according to the rules of displacement of tubes and the transducer enables proper rotation in 400 steps without jitter due to off-axis rotations.

A phantom is simulated with an inner diameter of

4 mm, an outer diameter of 7 mm and a height of 1 mm. The background of the medium (speed of sound = 1500 m s^{-1} , attenuation = 0 dB) has a homogeneous distribution of the mechanical properties ($E = 50 \text{ kPa}$, $\nu = 0.495$). The scatterers are distributed randomly in the phantom with constant bulk scatter density. The displacement of the scatterers due to overpressure in the phantom is calculated according to the rules of displacement for cylindrical tubes [6,7].

The ultrasound beam is generated from a circular transducer which is rotationally symmetric on the cross-sectional plane. The model makes use of the pulse-echo response model to calculate the impulse response [8,9]. The simulated ultrasound signal is sampled at 100 MHz.

The simulation is carried out for eccentricities of 0, 25, 50 and 75%. 25% eccentricity means that the source is positioned 25% out of the centre of the phantom. The pressure differences (the differences between inner and outer pressures of the tube) are taken 125, 250, 375 and 500 Pa. These pressure differentials correspond to strain values of 0.5, 1.0, 1.5 and 2.0%, respectively. These pressure differentials are used, because they result in strain values similar to those found in arteries due to blood pressure [10]. The values for the signal-to-noise ratio (SNR) are 10, 20 and 30 dB. The scatter density is 20×10^4 scatterers per 100 mm^3 . To investigate the influence of the used window for matching traces, window sizes of 0.5 and 1 μs were used.

In the simulations no rotational artefacts are present, which means that each angle in the first data set corresponds to each counterpart in the other data set. However, owing to an eccentric position of the catheter

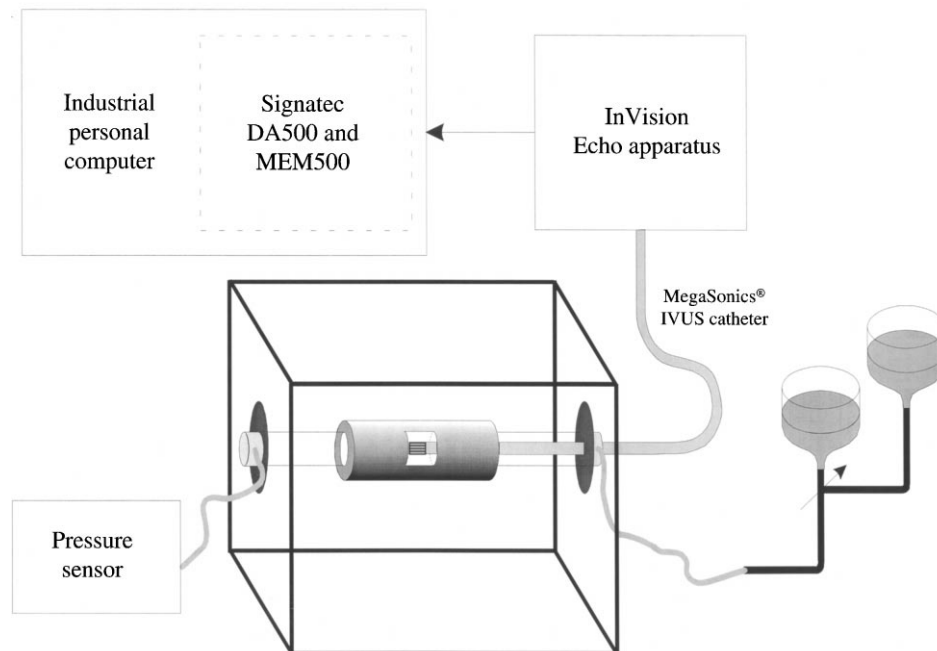


Fig. 2. The experimental set-up.

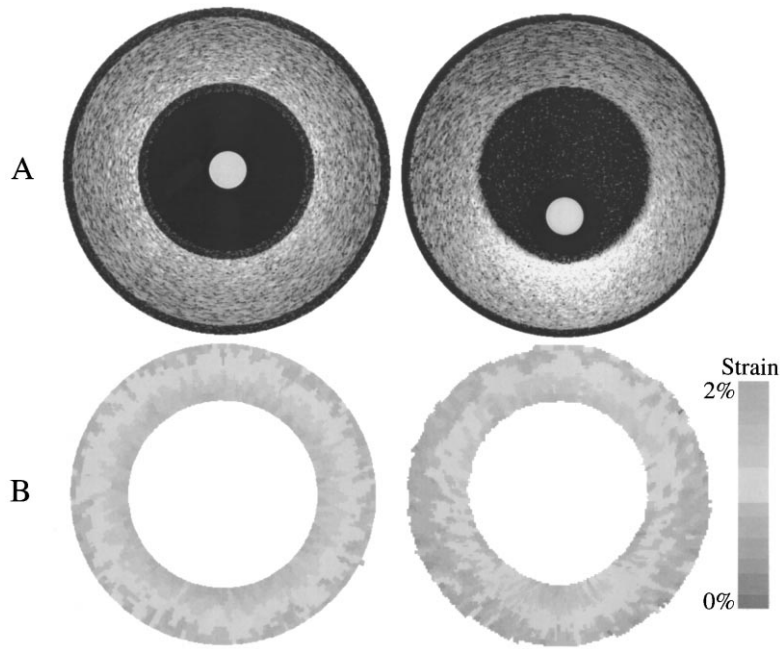


Fig. 3. (a) Simulated echograms and (b) corresponding elastograms for an eccentric position of the catheter of 0 and 50% (20×10^4 scatterers, SNR is 20 dB and 500 Pa pressure differential).

the direction of displacement of the tissue and the ultrasound beam are not always aligned. Since this effect can be described theoretically, the relation between traces before and after compression is known. The values of the displacements are clipped between -5 and 5 in discrete numbers, because only small displacements are investigated. To get an indication of which algorithm best matches the angles, the standard deviation of the angle displacements is taken as a figure of merit. The search algorithm with the smallest standard deviation performs best.

2.3. Experiments with a phantom

The in vitro measurements were performed in a water tank (Fig. 2) with a MegaSonics array transducer (EndoSonics, Rijswijk, The Netherlands). For the medium a layered phantom is used. With these experiments the following artefacts are minimised. By using the balloon that is positioned proximal to the transducer, the catheter is forced in a centric position in the phantom. Additionally, a non-rotating 64-element circular array transducer minimises rotational artefacts of the catheter. A sample frequency of 100 MHz is used. The search algorithms are also used to calculate the angle displacements and the standard deviation is also taken as a figure of merit for the performance of the algorithms.

3. Results

Echograms as produced with the simulations with an eccentric position of the catheter of 0 and 50% are

plotted in Fig. 3(a). The corresponding elastograms of these simulations are plotted in Fig. 3(b). It can be seen that an eccentric position of the catheter results in an underestimation of the strain in certain regions.

3.1. Results of simulation

In Fig. 4, the influence of the pressure difference on the performance of the algorithms is visualised. In these simulations the SNR was 20 dB and a window size of $1.0 \mu\text{s}$ was used. The tendency of the plots is that the standard deviation increases with increasing pressure

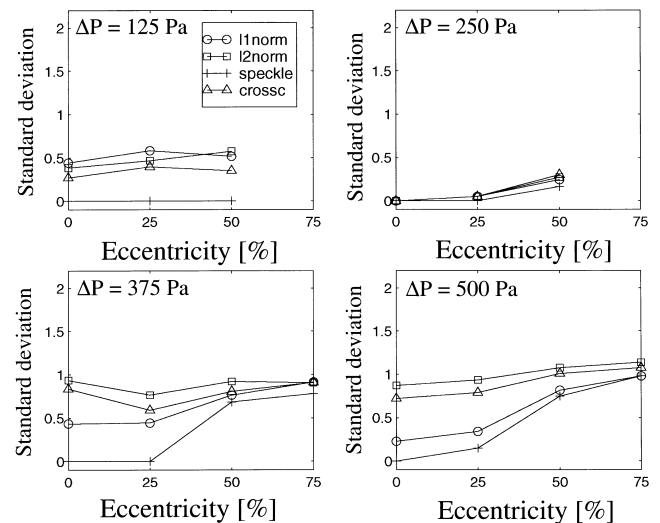


Fig. 4. Standard deviation for four pressure differentials as function of the position of the catheter (SNR = 20 dB, $T = 1 \mu\text{s}$).

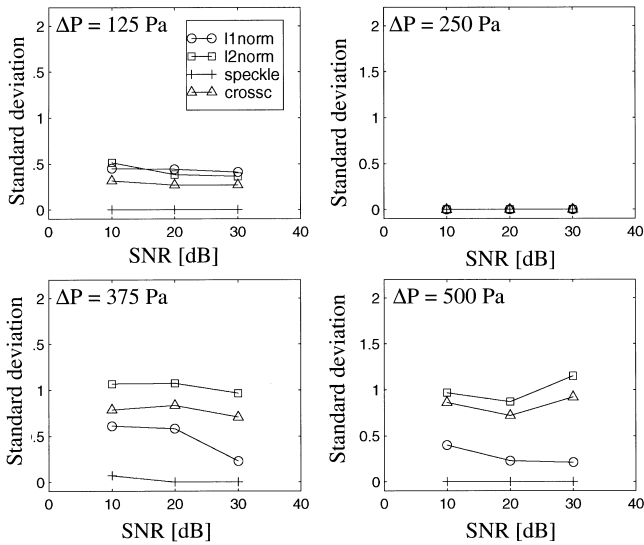


Fig. 5. Standard deviation for four pressure differentials as function of the SNR ($\Delta P = 125$ Pa, $T = 1 \mu s$).

difference. The speckle tracking algorithm gives the best results in all the subplots.

In Fig. 5, the results of the simulation for varying SNR are presented. For all SNRs, the speckle tracking algorithm has the best performance. The other three methods give similar results. The SNR is of minor influence on the four methods.

The results of the simulations in which the window size is varied (0.5 and $1.0 \mu s$) are presented in Fig. 6. The standard deviations obtained with a window size of $0.5 \mu s$ are larger than those obtained with a window size of $1.0 \mu s$. In both cases the speckle tracking algorithm gives the lowest standard deviations. This method is hardly affected by the window size, contrary to the other methods.

3.2. Results of experiments

In Fig. 7, the results of the four algorithms for the phantom experiment are presented. On the x -axis the angles are displayed. The relative angle displacement for each angle is plotted in the y -direction. As can be observed, the rotational artefacts are minimal since the

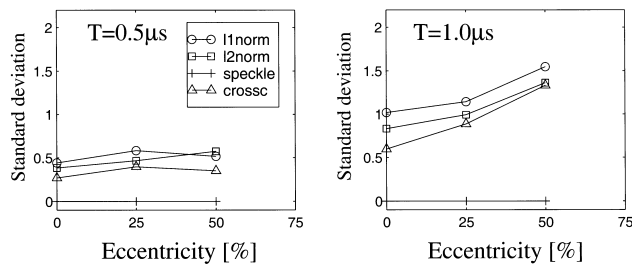


Fig. 6. Standard deviation for two window sizes as function of the position of the catheter (SNR = 20 dB, $\Delta P = 125$ Pa).

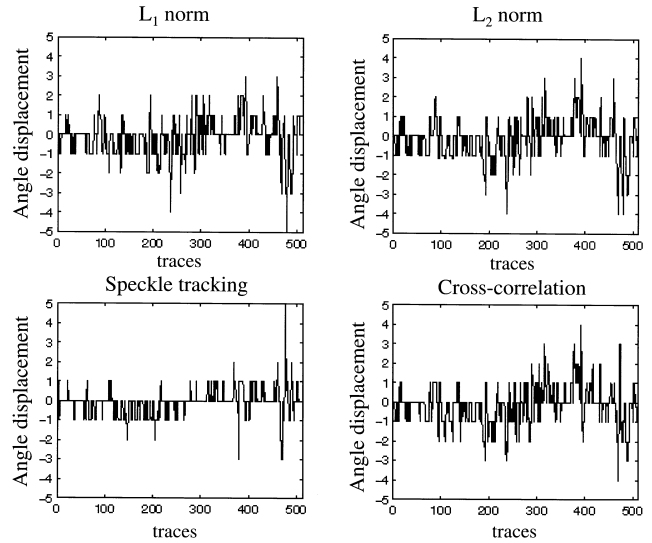


Fig. 7. Angle displacement of an in vitro measurement with an EndoSonics catheter on a phantom. A depth of 50 sample points and a window size of 100 sample points are used to obtain angle displacements. The pressure difference is obtained with a low pressure of 50 mmHg and a high pressure of 55 mmHg.

Table 1

Standard deviation of the angle difference for the four algorithms

Search algorithm	Standard deviation
l_1 norm	0.98
l_2 norm	1.04
speckle tracking	0.69
cross-correlation	1.02

relative angle displacements are mainly distributed along zero. In Table 1, the standard deviations of Fig. 7 are given.

4. Discussion

A search algorithm has to find which angles correspond to each other at two different pressures. In this study, the performance of four search algorithms was investigated. Using simulations and phantom experiments, the influence of the position of the catheter in the lumen (eccentricity), the SNR, the rate of strain in the material and the size of the search window on the performance were investigated. The quality of the search algorithms was expressed in terms of the standard deviation of the measured angle displacements. The echograms as produced with the simulations are similar to echograms obtained with in vitro experiments [10]. In the elastograms, regions with an underestimation of the strain are observed. This underestimation is caused by the angle between ultrasound beam and the direction of the strain. In this particular geometry, the strain is always perpendicular to the boundary between lumen

and the vessel wall. An off-centre position causes an angle between strain and ultrasound beam. Additionally, an eccentric position causes a misalignment of the corresponding angles acquired at the low and high pressure. The theoretic difference between angles is visualised in Fig. 8(a) and (c). The difference as determined with one of the search algorithms is presented in Fig. 8(b) and (d). The difference can be described by a sine wave [10]. Since the performance of the algorithms is described by the standard deviation, the general tendency is that the standard deviation increases with increasing eccentricity.

The standard deviation also increases with increasing pressure differential. The correlation between two signals at different pressure differences decreases with higher pressure difference. This is due to the scaling of the medium and the fact that the pulse remains its shape. Because of this decorrelation, it is harder to match the corresponding windows with each other. It is remarkable that the pressure difference of 250 Pa at an eccentricity of 0% gives a standard deviation of zero for all the search algorithms. The reason for that can be explained as follows: the axial displacement can be any real number. However, for a pressure difference of 250 Pa the displacement as modelled in this study equals exactly five sample points. The other pressure differences do not give a displacement of an integer number of sample points. Because the displacement is expressed in an integer, a search algorithm has to choose between two windows that do not sufficiently resemble the window at low pressure.

Looking at the results as a function of the SNR, it can be seen that the standard deviation is hardly influenced by the SNR. Only in the case of a window size of 0.5 μs does the standard deviation decrease with

better SNR. Again speckle tracking has the best performance. In fact this algorithm acts as a sort low pass filter. The speckle tracking algorithm takes the envelope of the r.f. signal. Because the envelope is much better sampled than the r.f. signal, the speckle tracking algorithm is less sensitive to the positions of the sample points. The speckle tracking algorithm searches more globally than the other methods and is not very sensitive to noise. Although this algorithm is less suitable for strain estimation, it gives the best performance for matching corresponding regions.

The window sizes were chosen as 0.5 and 1.0 μs . In general, a larger window size produces better results. A larger window has a more nearly unique signal than a smaller window. It contains more information than a small window. The disadvantage of large windows is an increased computation time and reduced resolution.

Generally speaking the speckle tracking algorithm is the best method for finding the corresponding angles, because the signal is smoothed by this algorithm and the sampling is better as a result of taking the envelope of the signal.

5. Conclusions

It can be concluded that the speckle tracking algorithm has better performance than the other three methods. The other three methods give in general higher standard deviations, which are mutually comparable. For window sizes of 0.5 and 1.0 μs the speckle tracking algorithm performs well. In general a window size of 0.5 μs gives larger standard deviations than the window size of 100 points. The speckle tracking algorithm performs also well for all different SNRs (10–30 dB). For the various eccentricities, the speckle tracking algorithm does well again. It also can be seen that eccentricities of 50 and 75% give larger standard deviations than those of 25 and 0%.

By applying the search algorithms to measurements of in vitro results of a phantom with an array transducer, it appears that the speckle tracking algorithm also performs well. Because an array transducer is used, the rotational artefacts of the transducer are minimised. The angle displacement should be zero, but the actual angle displacements are not known.

Acknowledgement

This work was supported by the Dutch Technology Foundation (STW).

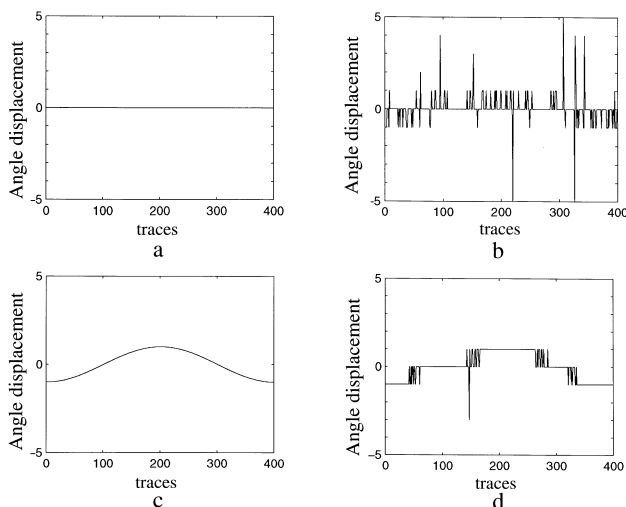


Fig. 8. Theoretical shift in angles and shift as determined with the speckle tracking method for an eccentric position of the catheter of (a, b) 0% and (c, d) 50%.

References

- [1] C.L. de Korte, A.F.W. van der Steen, E.I. Céspedes, G. Pasterkamp, Intravascular ultrasound elastography in human arteries: initial experience in vitro, *Ultrasound Med. Biol.* 24 (3) (1998) 401–408.
- [2] L.H. Bohs, G.E. Trahey, A novel method for angle independent ultrasonic imaging of blood flow and tissue motion, *IEEE Trans. Biomed. Eng.* 38 (3) (1991) 280–286.
- [3] A. Duijndam and G. Drijkoningen, *Parametric Inversion with Seismic Applications*, Delft University Press, Delft, 1996.
- [4] I.A. Hein, W.D. O'Brien, Current time-domain methods for assessing tissue motion by analysis from reflected ultrasound echoes: A review, *IEEE Trans. Ultrasonics Ferroelectr. Freq. Control* 40 (2) (1993) 85–102.
- [5] M. Parrilla, J.J. Anaya, C. Fritsch, Digital signal processing techniques for high accuracy ultrasonic range measurements, *IEEE Trans. Instrum. Meas.* 40 (3) (1991).
- [6] A.E.H. Love, *A Treatise on the Mathematical Theory of Elasticity*, Dover Publications, New York, 1944.
- [7] C.L. de Korte, E.I. Céspedes, A.F.W. van der Steen, C.T. Lancée, Intravascular elasticity imaging using ultrasound: feasibility studies in phantoms, *Ultrasound Med. Biol.* 23 (5) (1997) 735–746.
- [8] W. Li, *Image and signal processing in intravascular ultrasound*, Ph.D. Thesis, Erasmus University Rotterdam, 1997.
- [9] J.A. Jensen, *Estimation of Blood Velocities Using Ultrasound*, Cambridge University Press, Cambridge, 1996.
- [10] C.L. de Korte, E.I. Céspedes, A.F.W. van der Steen, Influence of catheter position on estimated strain in intravascular elastography, *IEEE Trans. Ultrasonics Ferroelectr. Freq. Control* 46 (3) (1999) 616–625.